



Adipophilin expression in cutaneous malignant melanoma is associated with high proliferation and poor clinical prognosis

Masakazu Fujimoto¹ · Ibu Matsuzaki¹ · Kazuchika Nishitsuji^{1,2} · Yuki Yamamoto³ · Daisuke Murakami⁴ · Takanori Yoshikawa⁵ · Ayaka Fukui¹ · Yuuki Mori¹ · Masaru Nishino¹ · Yuichi Takahashi¹ · Yoshifumi Iwahashi¹ · Kenji Warigaya¹ · Fumiyoshi Kojima¹ · Masatoshi Jinnin³ · Shin-ichi Murata¹

Received: 21 August 2019 / Revised: 1 November 2019 / Accepted: 12 November 2019 / Published online: 19 December 2019
© The Author(s), under exclusive licence to United States and Canadian Academy of Pathology 2019

Abstract

Adipophilin (ADP) is a primary protein component of lipid droplets (LDs). For more than half a century, certain types of cancer cells have been known to contain LDs in their cytoplasm. However, the pathological significance of ADP or LDs in cancer remains unclear. In the present study, we investigated the association between ADP and other pathological characteristics in cutaneous malignant melanomas to clarify the role of ADP in melanoma cells. We immunostained whole paraffin sections of primary cutaneous melanomas obtained from 90 cases for ADP, after which we analyzed the correlation between ADP immunohistochemistry (IHC) and patient survival data. We also studied the relationship between the ADP IHC score and in situ hybridization (ISH) score of ADP mRNA, and the Ki67-labeling index (Ki67-LI) by using tissue microarrays consisting of 74 primary cutaneous malignant melanomas, 19 metastasizing melanomas, and 29 melanocytic nevi. Finally, we analyzed the relationship between ADP expression and cell proliferation in cutaneous melanoma cell lines. We found that high ADP expression was associated with poor metastasis-free survival, disease-specific survival, and overall survival rates of patients with cutaneous melanomas ($P < 0.05$). By linear regression analysis, ADP IHC was correlated with increasing ADP mRNA ISH H-scores and Ki67-LI scores in melanocytic lesions ($P < 0.01$). ADP IHC and ADP ISH H-scores and Ki67-LI scores were greater in pT3–4 melanomas than in pT1–2 melanomas. In cell-based assays, cells with increased ADP expression showed higher proliferation rates compared with those of low-ADP cells. Thus, ADP expression in malignant melanoma was significantly associated with high cell proliferation and poor clinical prognosis. Our results thus indicate a significant association between ADP and melanoma progression, and we propose that ADP may be a novel marker of aggressive cutaneous melanoma with a lipogenic phenotype.

These authors contributed equally: Masakazu Fujimoto, Ibu Matsuzaki

✉ Masakazu Fujimoto
fujimasa@wakayama-med.ac.jp

✉ Kazuchika Nishitsuji
nishit@wakayama-med.ac.jp

¹ Department of Diagnostic Pathology, Wakayama Medical University, Wakayama, Japan

² Department of Biochemistry, Wakayama Medical University, Wakayama, Japan

³ Department of Dermatology, Wakayama Medical University, Wakayama, Japan

⁴ Second Department of Surgery, Wakayama Medical University, Wakayama, Japan

⁵ Clinical Study Support Center, Wakayama Medical University, Wakayama, Japan

Introduction

In cancers, the Warburg effect, or aerobic glycolysis, results in efficient biomass synthesis including lipid synthesis that is required for aggressive cell proliferation [1–3]. For more than 50 years, certain types of cancer cells have been documented to contain lipid droplets (LDs) in their cytoplasm [4, 5]. Until recently, intracellular LDs had been thought to be merely a result of excessive lipid levels; however, a number of studies have demonstrated the essential role of LDs in regulating lipid metabolism as dynamic organelles [6, 7].

LDs are coated by PAT (perilipin/ADRP/TIP47) family proteins [8]. Emerging evidence suggests a potential role of PAT proteins in various pathological conditions including cancer progression [8–10]. Overexpression of adipophilin (ADP), also known as perilipin 2 or adipose differentiation-related protein, has been reported in various cancer types

[11–24]. Indeed, we and others recently described increased ADP expression in malignant melanoma [25–27], which is one of the most aggressive skin cancers with enhanced lipid metabolism [28, 29]. However, the pathological significance of ADP expression in melanoma remains to be elucidated. In the present study, we analyzed the correlation between ADP and melanoma cell proliferation and patient survival data. Our study develops and deepens previous understanding of ADP in cutaneous melanomas.

Materials and methods

Selection of patients and histopathological evaluation

The Institutional Ethics Committee granted approval for this retrospective study (No. 1757). Between January 2001 and March 2017, 100 consecutive patients with primary cutaneous malignant melanoma underwent surgical resection at Wakayama Medical University Hospital. Paraffin blocks were available for 93 of these 100 patients and were used in the present study. In addition, 24 metastasizing melanomas from 22 patients were extracted for tissue microarray (TMA) construction. Among these 22 patients with metastasizing melanomas, 14 primary tumors were involved in the primary melanoma group described above; the primary tumors of the other eight patients were only biopsied, or resected at outside hospitals, thus were not included in the current study. Furthermore, 30 melanocytic nevi from different patients who underwent resection during the same period were randomly selected for TMA. Patients' follow-up data and clinical information were retrieved from the patients' charts. All resected specimens were fixed with formalin, sectioned, and stained with hematoxylin and eosin in the conventional manner. All glass slides were reviewed by MF for pathological parameters; nucleoli visible at $\times 100$ magnification was defined as conspicuous nucleoli in this study [30]. All cases were staged according to the 8th Union for International Cancer Control TNM classification [31].

TMA

Ninety-two primary cutaneous melanomas, 24 metastasizing melanomas, and 30 melanocytic nevi were included in TMAs. TMAs were constructed in a manner described previously [20]. Briefly, for all cases, the most morphologically representative tumor region was determined on the basis of hematoxylin and eosin-stained slides. For TMA construction, one tissue core with a diameter of 2 mm was punched out from each donor tumor block with a thin-walled stainless steel needle (Azumaya, Tokyo, Japan), after which it was arrayed in a recipient paraffin block.

Cell culture

C32TG and HMY-1 human cutaneous melanoma cells and HuH7 human hepatocellular carcinoma cells were obtained from the JCRB Cell Bank (Osaka, Japan). C32TG cells were cultured in Eagle's medium (Wako Pure Chemical Industries, Osaka, Japan) with 10% fetal bovine serum (Biowest, Nuaille, France). HMY-1 cells and HuH7 cells were maintained in Dulbecco's modified Eagle's medium (Nacalai Tesque, Kyoto, Japan) with 10% fetal bovine serum. All cells were maintained at 37 °C in a 5% CO₂ atmosphere. To investigate cell proliferation and lipid accumulation, C32TG and HMY-1 cells were cultured with various concentrations of glucose (0, 0.25, or 1.0 g/L) for 24–48 h. LDs were visualized by means of oil red O staining according to the manufacturer's procedure (Muto Pure Chemicals Co. Ltd., Tokyo, Japan). HuH7 cells were used as a positive control for oil red O staining [32]. Paraffin-embedded cell blocks for immunohistochemistry (IHC) were prepared by using the fixed sediment method. Briefly, cells were harvested, placed into 15-mL tubes, and centrifuged at 1000 *g* for 3 min. The supernatant was removed, after which the resultant pellet was fixed with 10% formalin for 24 h. After formalin was removed, the tip of the tube containing the cell pellet was cut off with a blade and processed as tissue. Then the paraffin-infiltrated cell pellet was removed from the tip of the tube and embedded in a paraffin block. These cell blocks were sectioned and immunostained as described below.

Cell proliferation assay

C32TG and HMY-1 melanoma cells were plated at densities of 4.0×10^4 cells/cm² with glucose concentrations of 1.0, 0.25, or 0 g/L in 96-well plates. Cell viability was quantitatively determined by using the WST-1 cell proliferation assay (Roche, Basel, Switzerland) according to the manufacturer's instructions. In brief, WST-1 (2-(4-iodophenyl)-3-(4-nitrophenyl)-5-(2,4-disulfophenyl)-2H-tetrazolium, monosodium salt) was added to each well for 0, 24, 48, and 72 h, after which cells were incubated for 2 h and cell viability was determined by measuring the absorbance at 450 nm with a Corona Microplate Reader (Hitachi, Tokyo, Japan).

Western blot analysis

Cells were plated on six-well culture plates and incubated in different glucose concentrations at 37 °C for 48 h. Whole-cell lysates were prepared by using the trichloroacetic acid precipitation method as previously described [33]. Briefly, cells were washed with phosphate-buffered saline three times and were then

treated with 10% (w/v) trichloroacetic acid in phosphate-buffered saline on ice for 30 min, after which samples were centrifuged at 1000 *g* for 5 min at 4 °C. The precipitates were dissolved in sodium dodecyl sulfate-polyacrylamide gel electrophoresis (SDS-PAGE) sample buffer [0.125 M Tris-HCl; 4% (w/v) SDS, 20% (v/v) glycerol, 12% (v/v) 2-mercaptoethanol, and 0.01% (w/v) bromophenol blue] to obtain whole-cell lysates. These lysates were subjected to SDS-PAGE with 10% gels and were transferred to polyvinylidene difluoride membranes (Millipore, Billerica, MA, USA). ADP on the membranes was probed with an anti-ADP antibody (LifeSpan Biosciences, Seattle, WA, USA) followed by a horseradish peroxidase-labeled anti-rabbit antibody (Cell Signaling Technology, Inc., Beverly, MA, USA) and ImmunoStar LD (Wako Pure Chemical Industries). For detection of phosphorylated Akt and extracellular-signal-regulated kinase 1/2 (ERK1/2), membranes were probed with a rabbit polyclonal anti-phosphorylated Akt antibody, rabbit monoclonal anti-pan Akt antibody, rabbit polyclonal anti-phosphorylated ERK1/2 antibody, or rabbit monoclonal anti-ERK1/2 antibody (Cell Signaling Technology, Beverly, MA, USA). Protein contents of cell lysates were normalized to actin expression levels. Signals were obtained by using a WSE-6100 LuminoGraph I (ATTO Corporation, Tokyo, Japan).

IHC

Immunostaining was performed by using an automated immunostainer with the standardized polymer-based detection system (Histostainer 48A, Nichirei, Tokyo, Japan; or Bond III, Leica Microsystems, Wetzlar, Germany), for ADP (AP125; Progen Biotechnik GmbH, Heidelberg, Germany) and Ki67 (MIB-1; Dako, Carpinteria, CA, USA). Red chromogen (Fast Red II Substrate Kit, Nichirei) was used for ADP staining on paraffin sections of surgically resected melanomas and cultured cells. Conventional DAB brown staining (Bond Polymer Refine detection kit, Leica Microsystems) with Giemsa counter stain was used for ADP staining on cell block sections of cultured melanoma cells. The specimens were examined with a light microscope. Sebaceous glands were used as built-in positive controls for ADP staining. ADP IHC staining in each tumor cell was evaluated by calculating the extent of the area of the tumor cell cytoplasm that was occupied by ADP-positive granules or vacuoles by means of a 0, 1+, 2+, and 3+ schema. Then scoring of ADP IHC was performed by using the H-score [(percentage at 1+) × 1+ (percentage at 2+) × 2+ (percentage at 3+) × 3]. The values for Ki67-positive tumor cells per 100 tumor cells were calculated separately for every core by focusing on a representative area for the Ki67-labeling index (Ki67-LI).

ISH

ADP mRNA ISH was performed with an ADP mRNA-specific probe and the RNAscope 2.5 HD-RED reagent kit (Advanced Cell Diagnostics, Newark, CA, USA) according to the manufacturer's protocol with some modifications. Briefly, sections were air-dried overnight, baked at 60 °C for 1 h, deparaffinized, and air-dried again. Glass slides were then boiled for 15 min in the target retrieval reagent and treated for 30 min with RNAscope Protease Plus at 40 °C before probe hybridization. Human peptidyl-prolyl cis-trans isomerase B (PPIB) and bacterial 4-hydroxy-tetrahydrodipicolinate reductase (*dapB*) probes were used as positive and negative controls, respectively. For hybridization, sections were incubated with each probe in an HybEZ oven (Advanced Cell Diagnostics) for 2 h at 408 °C. Signals were visualized by using the RNAscope 2.5 HD-RED reagent kit. Specimens with a higher intensity of punctate staining in the cytoplasm and nucleus than that of the signal on the *dapB*-negative control slide were regarded as having positive results. Scoring was performed by using the *H*-score as described above.

Statistical analyses

JMP Start Statistics version 13 (Statistical Discovery Software; SAS Institute, Cary, NC, USA) was used for statistical analyses. Comparisons between two groups were performed with Fisher's exact test or the Wilcoxon test to analyze categorical and continuous variables, respectively. The Kaplan–Meier method was used to evaluate metastasis-free, disease-specific, and overall survival rates, and log-rank tests were used to compare the groups. For metastasis-free survival, the first metastasis (regional or distant) was considered to be a failure. The Cox proportional hazards model was used to examine the relationship between clinicopathological parameters and survival. The Spearman rank correlation coefficient was calculated for the ADP ISH *H*-score and Ki67-LI scores against the ADP IHC *H*-score. Cell proliferation data were analyzed by one-way analysis of variance with Dunnett's test. A *P* value of <0.05 was said to be significant.

Results

Cohort characteristics

Because three slides did not contain sufficient tumor volume for evaluation, 90 primary melanomas were subjected to whole-section analysis. Table 1 provides the clinicopathological characteristics of the 90 patients. The mean age of patients at the time of surgery was 68.6 years

Table 1 Characteristics of patients and correlation between parameters and adipophilin (ADP) expression.

Parameter	<i>n</i>	%	High ADP	Low ADP	<i>P</i> value
Total	90	100	44	46	
Sex					
Male	45	50	23	22	0.8331
Female	45	50	21	24	
Age (years)					
<70	44	48.9	23	21	0.6734
≥70	46	51.1	21	25	
Stage					
I	31	34.4	6	25	<0.0001*
II	32	35.6	18	14	
III	21	23.3	17	4	
IV	6	6.7	3	3	
pT factor					
1	20	22.2	4	16	<0.0001*
2	13	14.4	3	10	
3	23	25.6	11	12	
4	34	37.7	26	8	
Histological type					
ALM	41	45.6	17	24	0.0644
SSM	25	27.8	12	13	
NM	19	21.1	14	5	
LMM	5	5.6	1	4	
Clark level					
II	13	14.4	3	10	0.072
III	5	5.6	1	4	
IV	55	61.1	29	26	
V	17	18.9	11	6	
Mitotic figures/mm ²					
≥1	66	73.3	40	26	0.0003*
0	24	26.7	4	20	
Ulceration					
Not identified	46	51.1	15	31	0.0029*
Present	44	48.8	29	15	
Regression					
Not identified	80	88.9	38	42	0.5175
Present	10	11.1	6	4	
Lymphovascular invasion					
Not identified	73	81.1	30	43	0.0027*
Present	17	18.9	14	3	
Perineural invasion					
Not identified	86	95.6	42	44	1
Present	4	4.4	2	2	
Tumor-infiltrating lymphocytes					
Minimal	44	48.9	24	20	0.4024
Non-brisk	31	34.4	12	19	
Brisk	15	16.7	8	7	

Table 1 (continued)

Parameter	<i>n</i>	%	High ADP	Low ADP	<i>P</i> value
Predominant cytology					
Epithelioid	66	73.3	33	33	0.8134
Spindled	24	26.7	11	13	
Nucleoli					
Conspicuous	53	58.9	37	16	<0.0001*
Inconspicuous	37	41.1	7	30	

**P* < 0.05

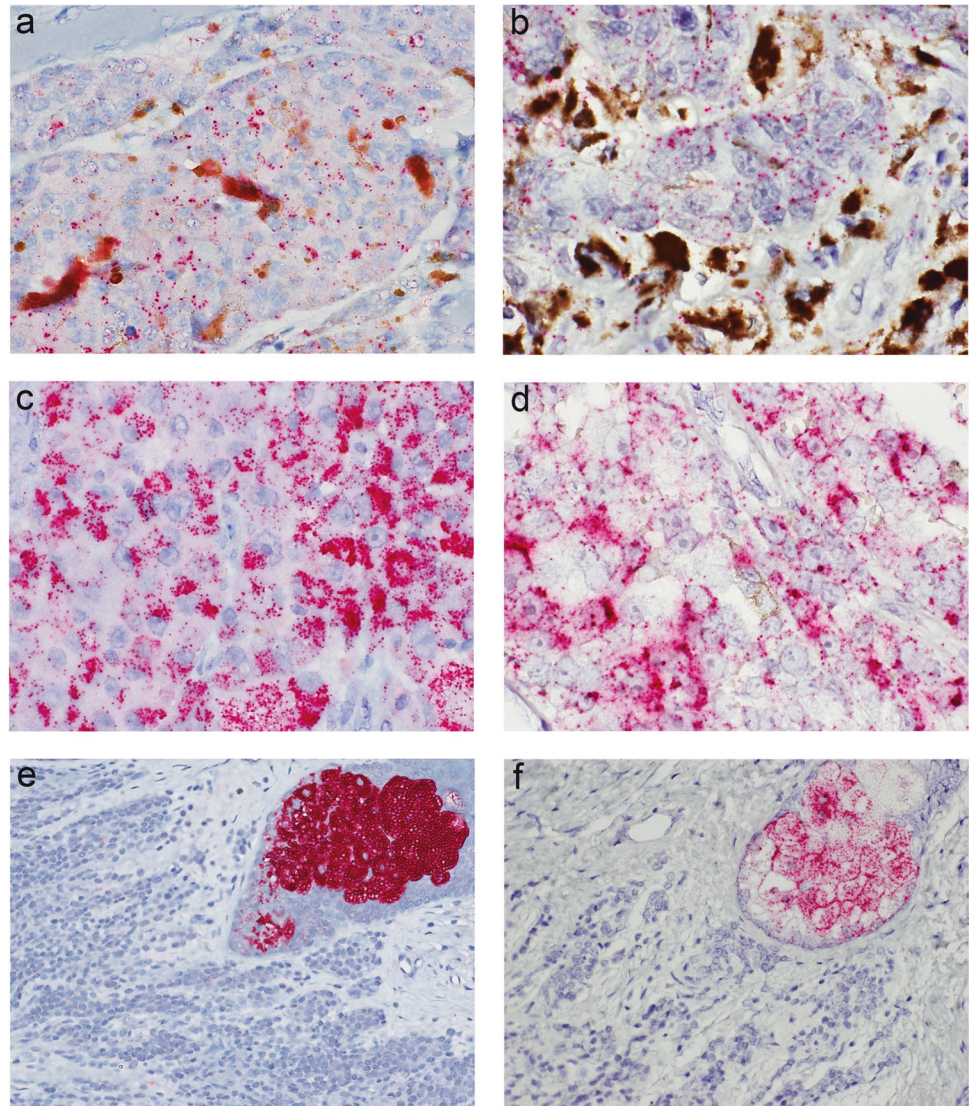
ALM acral lentiginous melanoma, LMM lentigo maligna melanoma, NM nodular melanoma, SSM superficial spreading melanoma

(range, 27–94 years). Among the 90 melanomas, about two-thirds were categorized as pT3 and pT4. Metastatic rates at the time of surgery were 0% (0/33) and 47.4% (27/57) for pT1-2 and pT3-4 melanomas, respectively (*P* < 0.0001). The mean follow-up period was 1821 days (range, 35–6273 days). Thirty-three (36.7%) patients died during the follow-up period. In TMAs, 24 cases were PPIB negative for mRNA ISH or did not contain sufficient tumor volume for evaluation. Consequently, the final analysis set of TMAs comprised 74 primary melanomas out of 90 on which whole section ADP IHC was performed, 19 metastasizing melanomas, and 29 melanocytic nevi.

Prognostic impact of ADP IHC in cutaneous melanomas

ADP IHC expression in cutaneous melanoma sections had a cytoplasmic and mostly granular staining pattern (Fig. 1). The ADP expression patterns were non-uniform, and no particular staining patterns were observed. *H*-scores of ADP IHC ranged from 0 to 250 (25% quartile, 20; median, 60; 75% quartile, 116.25). Median *H*-scores of 60 or lower and those higher than 60 were regarded as low and high ADP expression, respectively. High ADP expression was significantly correlated with the presence of mitotic figures (*P* = 0.003), ulceration (*P* = 0.0029), lymphovascular invasion (*P* = 0.0027), conspicuous nucleoli (*P* < 0.0001), pathological T factor (pT) (*P* < 0.0001), and tumor stage (*P* < 0.0001) (Table 1). The melanoma cells with high ADP expression tended to have a greater cytoplasmic volume without demonstrating “bubbly” or “frothy” cytoplasm. Figure 2 provides survival curves for high-ADP and low-ADP cases. Patients with high-ADP melanomas had significantly worse metastasis-free, disease-specific, and overall survival prognoses than patients with low-ADP melanomas (*P* < 0.0001, *P* = 0.0061, and *P* = 0.0119, respectively). However, this result did not occur in the multivariate Cox regression analysis (Table 2).

Fig. 1 Analysis of adipophilin (ADP) expression in primary cutaneous or metastatic melanomas. Representative case of primary cutaneous melanoma with high ADP immunohistochemistry (IHC) expression (a) and high ADP in situ hybridization (ISH) expression (b) as indicated by red signals, while melanin pigments appear in brown. High ADP IHC expression in metastatic melanoma (c) and ADP ISH expression in metastatic melanoma (d). Low ADP IHC expression in melanocytic nevus (e) and ADP ISH expression in melanocytic nevus (f). Sebaceous glands (upper right in e and f) are diffusely positive for ADP IHC with a globular staining pattern, and for ADP ISH with a granular staining pattern.



ADP IHC, ADP ISH, and Ki67-LI in TMAs

Median *H*-scores of ADP IHC and ADP ISH, and Ki67-LI scores in TMAs were 30 (range, 0–220), 5 (range, 0–260), and 20.5 (range, 0–83), respectively. The *H*-scores of ADP-IHC significantly correlated with ADP-ISH *H*-scores and Ki67-LI ($P < 0.0001$; Fig. 3a, b). The representative figures of ADP-ISH in melanocytic tumors with high and low ADP-IHC are shown in Fig. 1. Figure 3c–e illustrates that the median *H*-scores of ADP IHC increased in the order melanocytic nevi ($n = 29$), pT1-2 ($n = 25$), pT3-4 ($n = 49$), and metastasizing melanomas ($n = 19$); the actual corresponding scores were 10 (range, 0–40), 30 (range, 0–140), 60 (range, 0–180), and 70 (range, 0–200). All ADP IHC *H*-scores, ADP ISH *H*-scores, and Ki67-LI scores were significantly higher in pT3-4 melanomas than in pT1-2 melanomas ($P < 0.05$), which implies that ADP protein levels in melanoma cells may be correlated with

proliferative activity of the cells. No significant differences were observed between pT3-4 and metastatic melanomas. The results of ADP IHC *H*-scores in TMA (range, 0–220; median, 40) were lower than those of the whole section analysis (range, 0–250; median, 70), but the difference was not statistically significant ($p = 0.1445$).

ADP expression in melanoma cell lines

We investigated the relationship between cell proliferation and ADP levels by using human melanoma-derived cell lines—C32TG cells and HMY-1 cells. The proliferation assay with C32TG and HMY-1 melanoma cells showed that proliferation of these cells depended on glucose levels: cell proliferation increased in order of glucose concentrations of 0, 0.25, and 1.0 g/L (Fig. 4a). Cell proliferation at the glucose concentration of 1.0 g/L was significantly higher than that at 0 g/L and 0.25 g/L ($P < 0.05$). The Ki67-LI scores

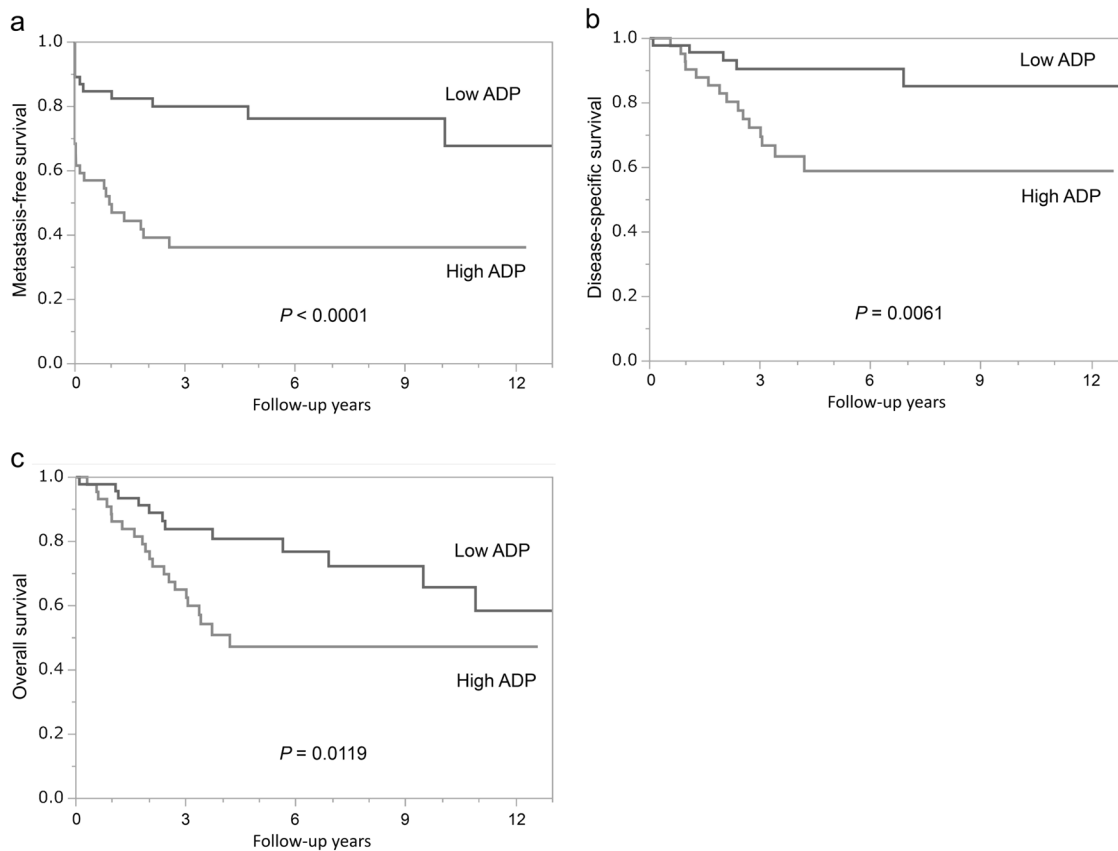


Fig. 2 Patients with high-adipophilin (ADP) melanoma had significantly worse metastatic-free, disease-specific, or overall survival. Kaplan–Meier survival curves for high-ADP and low-ADP cutaneous melanomas, with *P* values for metastasis-free (a), disease-specific (b), and overall (c) survival.

Table 2 Multivariate analysis of pathological parameters.

Parameter	MFS multivariate		DSS multivariate		OS multivariate	
	HR (95% CI)	<i>P</i>	HR (95% CI)	<i>P</i>	HR (95% CI)	<i>P</i>
pT (pT1-2 vs. pT3-4)	11.73 (4.22–34.81)	<0.0001*	2.14e + 9 (1.93–.)	0.0093*	1.74 (0.56–6.36)	0.35
Histological subtype (nodular vs. the other subtypes)	1.18 (0.54–2.61)	0.6662	0.95 (0.35–2.38)	0.9269	0.68 (0.27–1.55)	0.38
Mitotic figures, /mm ² (≥1 vs. 0)	3.59 (0.90–24.15)	0.071	7.74e + 8 (0.65–.)	0.105	1.88 (0.52–7.86)	0.34
Ulceration (present vs. not identified)	1.55 (0.68–3.92)	0.3007	0.99 (0.35–3.24)	0.9998	1.86 (0.77–4.99)	0.17
Lymphovascular invasion (present vs. not identified)	1.63 (0.75–3.51)	0.2106	1.32 (0.47–3.43)	0.5712	1.39 (0.59–3.10)	0.43
ADP (high vs. low)	1.52 (0.69–3.54)	0.2981	1.66 (0.59–5.41)	0.3389	1.34 (0.60–3.12)	0.47

*Statistically significant

CI confidence interval, DSS disease-specific survival, HR hazard ratio, MFS metastasis-free survival, OS overall survival

also increased with increasing glucose levels (Fig. 4b). ADP expression was highest in cells with the highest glucose concentration, as confirmed by IHC and Western blotting (Fig. 4c, d). The Akt pathway reportedly activated in ~70% of melanomas [34], and the ERK1/2 signaling is essential for the development and progression of melanoma [35]. Notably, activation of these kinases depended on the cellular lipid contents [36, 37]. Here, we further found that

both the Akt and ERK1/2 signaling were upregulated in melanoma cells cultured in the highest glucose concentration (Fig. 4d). In oil red O staining, only a few melanoma cells (<1%) were positive in contrast to ADP IHC in which all melanoma cells showed positive staining (Fig. 5a, b). In HuH7 hepatocytes used as a positive control for oil red O staining, ADP IHC showed diffusely positive patterns with wider positive areas than did oil red O staining (Fig. 5c, d).

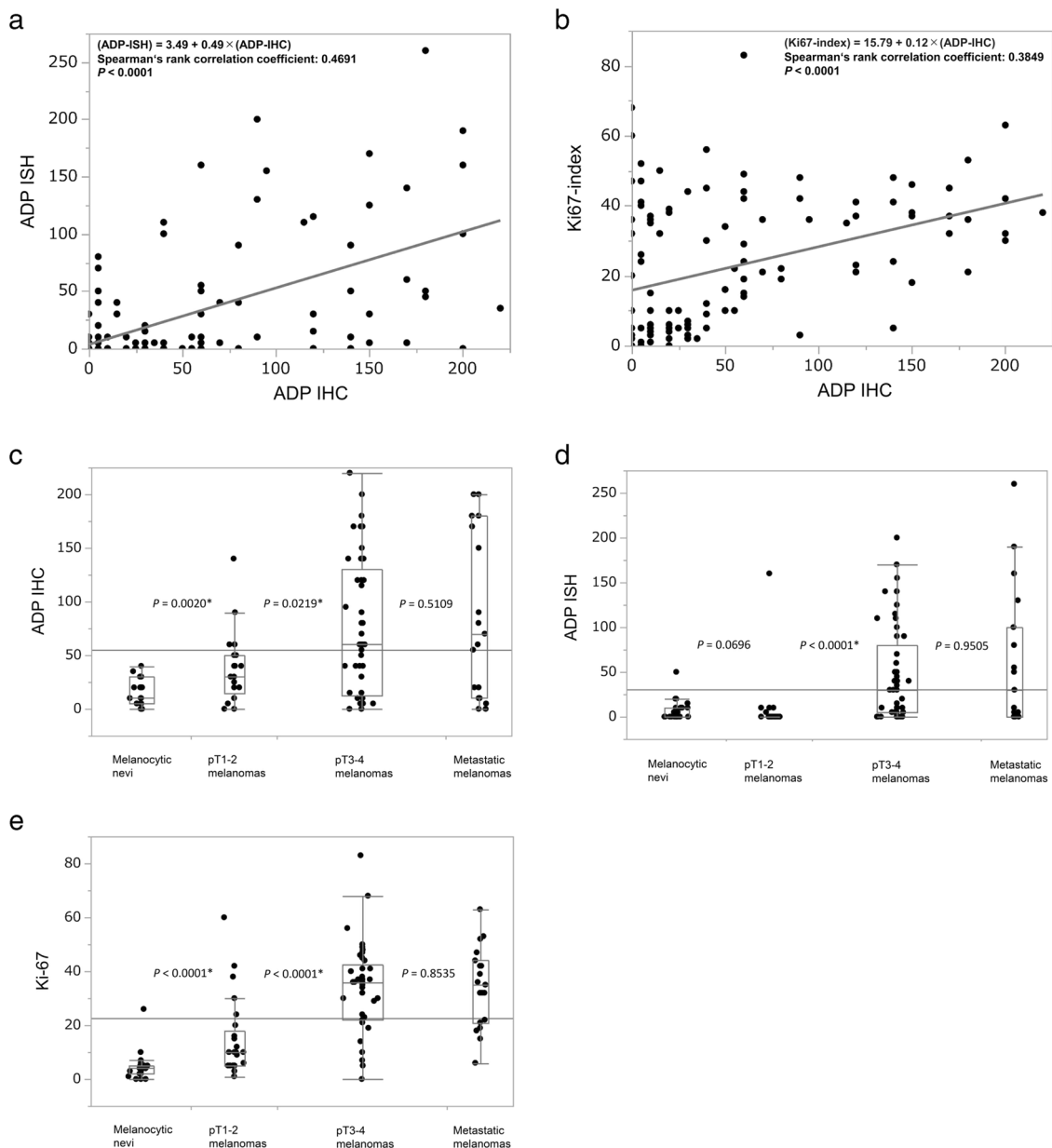


Fig. 3 Correlation analysis of median *H*-scores of adipophilin (ADP) immunohistochemistry (IHC) or ADP in situ hybridization (ISH) and Ki67-LI. ADP ISH *H*-score (a) and Ki67-LI score (b) versus ADP IHC *H*-score with *P* values of <0.0001. Comparison of the ADP IHC (c), ADP ISH (d), and Ki67-LI (e) *H*-scores in melanocytic nevi, pT1-2, pT3-4, and metastatic melanomas. All ADP IHC, ADP ISH, and Ki67 *H*-scores increased along with the progression of the disease from stage pT1-2 to stage pT3-4, with statistical

significance ($P = 0.0219$, $P < 0.0001$, and $P < 0.0001$, respectively), although no significant difference was observed between pT3-4 and metastatic melanomas ($P = 0.5109$, $P = 0.9505$, and $P = 0.8535$, respectively). A statistically significant difference was also observed between melanocytic nevi and pT1-2 melanomas in ADP IHC and Ki67-LI ($P = 0.0020$ and $P < 0.0001$, respectively) but not in ADP ISH ($P = 0.0696$).

Discussion

Detection of intracytoplasmic lipids in formalin-fixed paraffin-embedded tissues is difficult because lipids are removed during processing with xylene and ethanol. We and others have proposed that lipids can be analyzed indirectly by using immunohistochemical techniques with antibodies against the PAT family proteins that coat LDs,

especially ADP [19], which enables assessment of the contribution of LDs to tumor pathology. In fact, a number of reports have identified many types of ADP-positive tumors and suggested that ADP IHC results can be used as diagnostic or prognostic markers of these tumors. For example, ADP IHC positivity is believed to be a characteristic of sebaceous differentiation in cutaneous adnexal tumors [12, 17, 19], a marker for clear cell renal cell

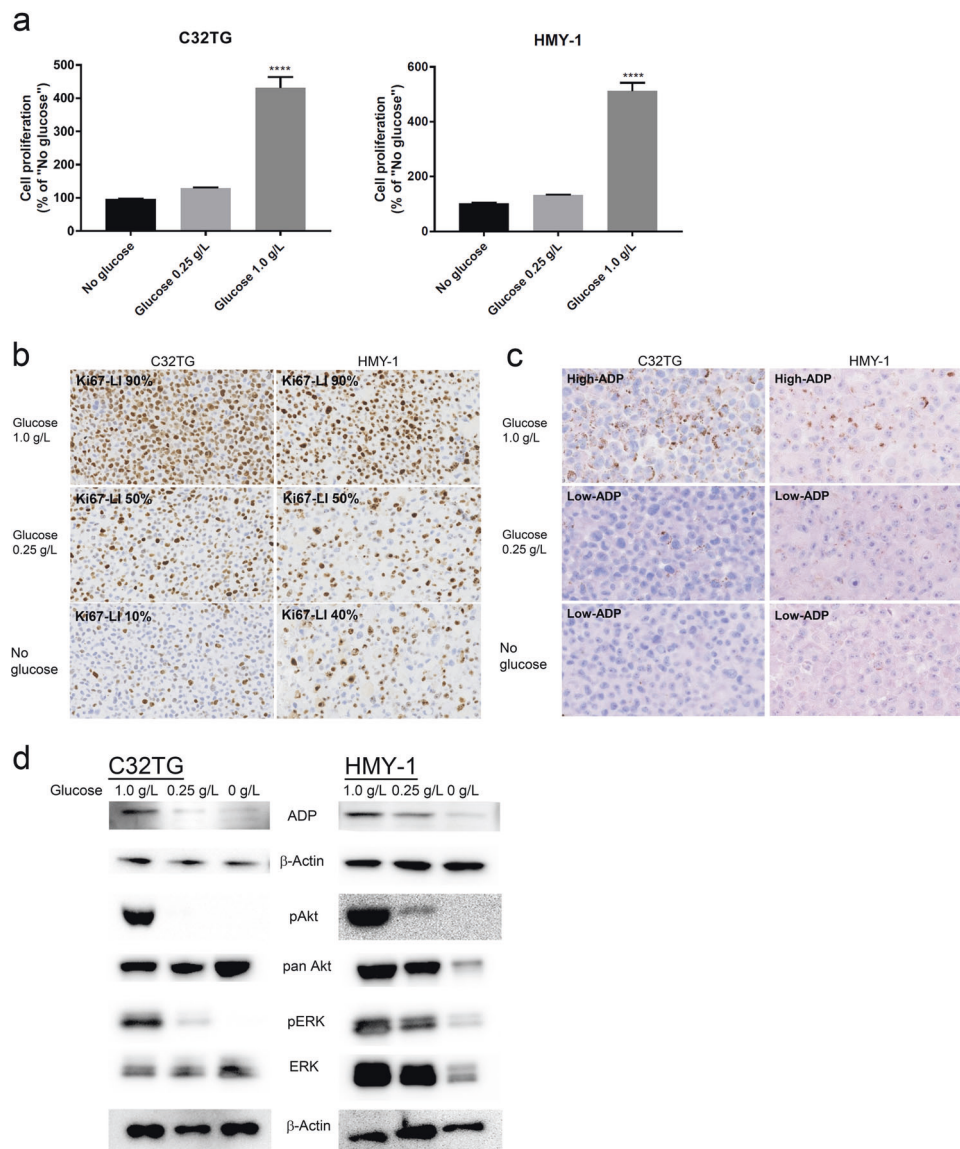


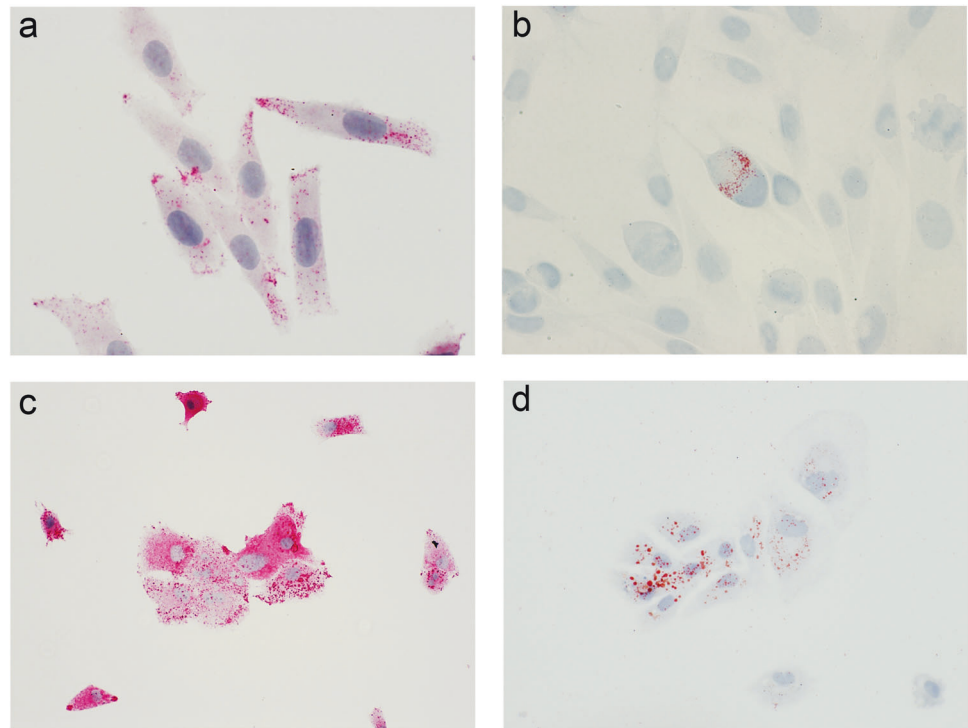
Fig. 4 Analysis of adipophilin (ADP) expression in and cell proliferation of human melanoma cells. a C32TG and HMY-1 melanoma cells were cultured at various glucose concentrations for 72 h, and proliferation was analyzed by using the WST assay. Proliferation of both melanoma cell lines increased in order of the glucose concentrations of 0, 0.25, and 1.0. Cell proliferation at the 1.0 g/L glucose concentration was significantly higher than that at the other concentrations ($P < 0.05$). **b** Melanoma cells were cultured at various glucose concentrations for 48 h, after which cells were stained by an anti-Ki67 antibody. The Ki67-LI of melanoma cells increased at

higher glucose concentrations. **c** Melanoma cells were cultured at various glucose concentrations for 24 h, after which cells were stained by an anti-ADP antibody. The staining was visualized by using a brown chromogen. ADP expression was highest at a glucose concentration of 1.0 g/L, as analyzed by immunohistochemistry (IHC). **d** ADP expression and phosphorylated Akt or ERK1/2 were analyzed by means of Western blotting, which confirmed higher ADP expression and phosphorylation of these kinases in melanoma cells cultured at higher glucose concentrations.

carcinoma and a predictor of this carcinoma's better prognosis [11, 23], a marker for Burkitt lymphoma [15], an indicator of apocrine differentiation in breast cancer [14], a characteristic of intestinal differentiation in gastric cancer [18], a feature of degenerative changes in thyroid cancer [21], and a negative prognostic indicator in lung and pancreatic adenocarcinomas [20, 22, 24]. Here, our comprehensive study investigated ADP expression in human

cutaneous melanoma tissues and confirmed that part of melanomas express ADP. The pattern of ADP expression observed here is more finely granular compared to that described for sebaceous lipid droplets. In practice, this staining pattern is usually interpreted as non-specific and not necessarily mentioned in relation to lipid metabolism per se. Actually, our study revealed a significant association between granular ADP staining and melanoma progression,

Fig. 5 Comparison of adipophilin (ADP) immunohistochemistry (IHC) with a red chromogen and oil red O staining. C32TG melanoma cells and HuH7 hepatocellular carcinoma cells were cultured with 1.0 g/L glucose for 24 h, after which ADP expression and lipid accumulation were analyzed by means of IHC and oil red O staining. All melanoma cells were positive for ADP IHC (a), whereas only a few melanoma cells were positive for oil red O staining (b). In HuH7 cells, ADP IHC (c) and oil red O staining (d) were both positive in a majority of the cells; the positive regions seen with ADP IHC were larger than those seen with oil red O staining.



which further suggests that granular ADP staining is not non-specific and rather reflects aggressive lipid metabolism in cancer cells [20, 22, 24]. As an unexpected result, ADP-positive melanoma cells in the current study clearly outnumbered oil red O-positive melanoma cells, which suggests that oil red O staining does not always correspond to granular ADP IHC staining (Fig. 5). ADP IHC in our study may have detected LDs, which are too small to study with a light microscope and oil red O staining [6]. Alternatively, ADP was reportedly concentrated at the site of LD biogenesis or ready reservoirs for rapid lipid packaging to LDs [38, 39]. Although a globular ADP IHC staining pattern highlights the contours of LDs [12], a granular ADP IHC staining pattern may have occurred because of non-LD-related ADP rather than ADP surrounding invisible LDs [6, 38]. This possibility should clearly be investigated. Nonetheless, our results strongly suggested that ADP expression in melanoma cells may reflect a requirement for a large mass of lipids that would lead to aggressive proliferation of melanomas with poor prognosis.

The mechanism by which ADP or LDs accumulated in tumor cells is not clear. The accumulation process and biological significance of LDs and ADP in human tumor cells seem to vary among tumor types [11–27]. In our study here, melanoma cell proliferation and ADP expression in melanoma cells were significantly correlated with and depended on glucose concentration. Cancer metabolism is characterized by increased glucose uptake and fermentation of glucose to lactate rather than complete oxidation of glucose in the

mitochondria even in aerobic conditions, that is, the Warburg effect [1–3]. This peculiar glucose metabolism observed in proliferating cancer cells results in efficient biomass synthesis including synthesis of lipids, which comprise plasma and organelle membranes of new daughter cells [1, 40]. Our observations suggest that ADP accumulation in human cutaneous melanoma is related to upregulation of lipogenesis via the Warburg effect. Summarizing the above, ADP expression may reflect increased lipid synthesis caused by enhancement of glucose uptake to meet the lipid requirement for cell membrane synthesis in proliferating melanoma cells rather than storing excess lipids due to decreased fat utilization.

The median scores of ADP IHC, ADP ISH, and Ki67 were higher in pT3–4 melanomas than in pT1–2 melanomas, whose metastatic rate was also higher than that of pT1–2 melanomas. The scores of pT3–4 melanomas were similar to those of metastatic melanomas, and previous immunohistochemical studies have shown that ADP is highly expressed in metastatic melanomas [25–27]. Moreover, fatty acid synthase, which is a key enzyme in fatty acid production, was reportedly upregulated, along with increasing Breslow tumor thickness, and showed high levels of expression in metastatic melanomas [28, 29]. Because fatty acids can be esterified with cholesterol or triglycerol to form cholesteryl esters or triglycerides that are stored as LDs, our results described here support the pathological importance of LD formation in human melanoma. CD36 is a scavenger receptor that is involved in the uptake of lipids including cholesterol and fatty acids from the extracellular

environment [41, 42]. CD36 is reportedly associated with melanoma metastasis [43, 44]). These lines of evidence indicate high metastatic activity of melanomas with a lipogenic phenotype [1]. In fact, notwithstanding the small sample size and limited follow-up period, we showed here that melanomas with high ADP expression demonstrated a significantly poor metastasis-free survival rate along with poor disease-specific and overall survival rates. Our observation of activation of the Akt and ERK1/2 signaling in melanoma cells with ADP accumulation suggests an additional role of cellular lipid storage in tumor growth, such as upregulation of several survival-related signaling pathways.

Regardless of recent progress in treatment, the 5-year overall survival rate remains below 50% in patients with advanced melanoma [45]. Enzymes and proteins that are involved in lipid metabolism have been identified as treatment targets in cancers including melanomas [40, 46, 47]. The fatty acid synthase inhibitor TVB-2640 has been in clinical trials for several cancers, with positive responses [48]. In view of the significant relationship between ADP and poor prognosis in cutaneous melanomas, ADP may be a new target for suppressing tumor progression, or a marker for predicting sensitivity to inhibition of lipid synthesis for optimal treatment planning or selection of patients.

As expected for the Asian population, acral lentiginous melanoma was overrepresented with the current cohort. However, the histological types did not show significant correlation with high ADP expression, while nodular melanoma tended to show high ADP expression ($P = 0.0644$, Table 1). Cytomorphologically, high ADP expression in melanoma cells was associated with prominent nucleoli. In an earlier study, distinct nucleoli in melanoma cells were related to an unfavorable prognosis in patients with cutaneous melanoma [49]. This relationship is reasonable because the nucleolus is a site of ribosome biogenesis, which is essential for protein synthesis and cell proliferation. Distinct nucleoli with a relatively greater volume of cytoplasm may be a common cytologic feature of cancers with a lipogenic phenotype [20]) and may reflect a requirement for ADP in melanoma cell proliferation.

In summary, we found that high ADP expression in cutaneous malignant melanoma was associated with high cell proliferation and poor prognosis, findings that support the high metastatic activity of melanomas with a lipogenic phenotype. Our results suggest that ADP may serve as a novel marker of aggressive cutaneous melanoma. Additional research is warranted to elucidate the mechanism of ADP accumulation and the relationship of ADP to metastatic activity of cutaneous melanomas.

Acknowledgements This work was supported by JSPS KAKENHI Grant Number JP17K15650. We thank Saeka Ikoma for her technical assistance.

Compliance with ethical standards

Conflict of interest The authors declare that they have no conflict of interest.

Publisher's note Springer Nature remains neutral with regard to jurisdictional claims in published maps and institutional affiliations.

References

- Menendez JA, Lupu R. Fatty acid synthase and the lipogenic phenotype in cancer pathogenesis. *Nat Rev Cancer*. 2007;7:763–77.
- Pavlova NN, Thompson CB. The emerging hallmarks of cancer metabolism. *Cell Metab*. 2016;23:27–47.
- Liberti MV, Locasale JW. The Warburg Effect: how does it benefit cancer cells? *Trends Biochem Sci*. 2016;41:211–8.
- Aboumrad MH, Horn RC Jr, Fine G. Lipid-secreting mammary carcinoma. Report of a case associated with Paget's disease of the nipple. *Cancer*. 1963;16:521–5.
- Wright DH. Lipid content of malignant lymphomas. *J Clin Pathol*. 1968;21:643–9.
- Ohsaki Y, Suzuki M, Fujimoto T. Open questions in lipid droplet biology. *Chem Biol*. 2014;21:86–96.
- Barbosa AD, Savage DB, Sinioglou S. Lipid droplet-organelle interactions: emerging roles in lipid metabolism. *Curr Opin Cell Biol*. 2015;35:91–97.
- Conte M, Franceschi C, Sandri M, et al. Perilipin 2 and age-related metabolic diseases: a new perspective. *Trends Endocrinol Metab*. 2016;27:893–903.
- Tirinato L, Pagliari F, Limongi T, et al. An overview of lipid droplets in cancer and cancer stem cells. *Stem Cells Int*. 2017;2017:1656053.
- Zhang P, Meng L, Song L, et al. Roles of perilipins in diseases and cancers. *Curr Genom*. 2018;19:247–57.
- Yao M, Tabuchi H, Nagashima Y, et al. Gene expression analysis of renal carcinoma: adipose differentiation-related protein as a potential diagnostic and prognostic biomarker for clear-cell renal carcinoma. *J Pathol*. 2005;205:377–87.
- Ostler DA, Prieto VG, Reed JA, et al. Adipophilin expression in sebaceous tumors and other cutaneous lesions with clear cell histology: an immunohistochemical study of 117 cases. *Mod Pathol*. 2010;23:567–73.
- Straub BK, Herpel E, Singer S, et al. Lipid droplet-associated PAT-proteins show frequent and differential expression in neoplastic steatogenesis. *Mod Pathol*. 2010;23:480–92.
- Moritani S, Ichihara S, Hasegawa M, et al. Intracytoplasmic lipid accumulation in apocrine carcinoma of the breast evaluated with adipophilin immunoreactivity: a possible link between apocrine carcinoma and lipid-rich carcinoma. *Am J Surg Pathol*. 2011;35:861–7.
- Ambrosio MR, Piccaluga PP, Ponzoni M, et al. The alteration of lipid metabolism in Burkitt lymphoma identifies a novel marker: adipophilin. *PLoS ONE*. 2012;7:e44315.
- Boussahmain C, Mochel MC, Hoang MP. Perilipin and adipophilin expression in sebaceous carcinoma and mimics. *Hum Pathol*. 2013;44:1811–6.
- Milman T, Schear MJ, Eagle RC Jr. Diagnostic utility of adipophilin immunostain in periocular carcinomas. *Ophthalmology*. 2014;121:964–71.
- Gushima R, Yao T, Kurisaki-Arakawa A, et al. Expression of adipophilin in gastric epithelial neoplasia is associated with

- intestinal differentiation and discriminates between adenoma and adenocarcinoma. *Virchows Arch.* 2016;468:169–77.
19. Plaza JA, Mackinnon A, Carrillo L, et al. Role of immunohistochemistry in the diagnosis of sebaceous carcinoma: a clinicopathologic and immunohistochemical study. *Am J Dermatopathol.* 2015;37:809–21.
 20. Fujimoto M, Yoshizawa A, Sumiyoshi S, et al. Adipophilin expression in lung adenocarcinoma is associated with apocrine-like features and poor clinical prognosis: an immunohistochemical study of 328 cases. *Histopathology.* 2017;70:232–41.
 21. Takada N, Hirokawa M, Ito A, et al. Cytoplasmic lipid accumulation characteristic of the cribriform variant of papillary thyroid carcinoma. *Pathobiology.* 2017;84:251–7.
 22. Shin SA, Na HY, Choe JY, et al. The expression of adipophilin is frequently found in solid subtype adenocarcinoma and is associated with adverse outcomes in lung adenocarcinoma. *J Pathol Transl Med.* 2018;52:357–62.
 23. Cao Q, Ruan H, Wang K, et al. Overexpression of PLIN2 is a prognostic marker and attenuates tumor progression in clear cell renal cell carcinoma. *Int J Oncol.* 2018;53:137–47.
 24. Hashimoto Y, Ishida M, Ryota H, et al. Adipophilin expression is an indicator of poor prognosis in patients with pancreatic ductal adenocarcinoma: an immunohistochemical analysis. *Pancreatol.* 2019;19:443–8.
 25. Fujimoto M, Matsuzaki I, Yamamoto Y, et al. Adipophilin expression in cutaneous malignant melanoma. *J Cutan Pathol.* 2017;44:228–36.
 26. Fiorentzis M, Kalirai H, Katopodis P, et al. Adipophilin expression in primary and metastatic uveal melanoma: a pilot study. *Graefes Arch Clin Exp Ophthalmol.* 2017;255:1049–51.
 27. Alexandre G, Egal E, Shinomia S, et al. Adipophilin expression in the progression of melanomas. *Am J Clin Pathol.* 2018;149:S13–S33.
 28. Innocenzi D, Alo PL, Balzani A, et al. Fatty acid synthase expression in melanoma. *J Cutan Pathol.* 2003;30:23–28.
 29. Kapur P, Rakheja D, Roy LC, et al. Fatty acid synthase expression in cutaneous melanocytic neoplasms. *Mod Pathol.* 2005;18:1107–12.
 30. Fuhrman SA, Lasky LC, Limas C. Prognostic significance of morphologic parameters in renal cell carcinoma. *Am J Surg Pathol.* 1982;6:655–63.
 31. Brierley JD, Gospodarowicz MK, Wittekind C. *TNM classification of malignant tumours.* Singapore: Wiley-Blackwell; 2017.
 32. Fujimoto Y, Itabe H, Sakai J, et al. Identification of major proteins in the lipid droplet-enriched fraction isolated from the human hepatocyte cell line HuH7. *Biochim Biophys Acta.* 2004;1644:47–59.
 33. Niikura Y, Nonaka T, Imajoh-Ohmi S. Monitoring of caspase-8/FLICE processing and activation upon Fas stimulation with novel antibodies directed against a cleavage site for caspase-8 and its substrate, FLICE-like inhibitory protein (FLIP). *J Biochem.* 2002;132:53–62.
 34. Cheung M, Sharma A, Madhunapantula SV, et al. Akt3 and mutant V600E B-Raf cooperate to promote early melanoma development. *Cancer Res.* 2008;68:3429–39.
 35. Savoia P, Fava P, Casoni F, et al. Targeting the ERK signaling pathway in melanoma. *Int J Mol Sci.* 2019;20:1483.
 36. Zhuang L, Lin J, Lu ML, et al. Cholesterol-rich lipid rafts mediate akt-regulated survival in prostate cancer cells. *Cancer Res.* 2002;62:2227–31.
 37. Ringerike T, Blystad FD, Levy FO, et al. Cholesterol is important in control of EGF receptor kinase activity but EGF receptors are not concentrated in caveolae. *J Cell Sci.* 2002;115(Pt 6):1331–40.
 38. Robenek H, Hofnagel O, Buers I, et al. Adipophilin-enriched domains in the ER membrane are sites of lipid droplet biogenesis. *J Cell Sci.* 2006;119(Pt 20):4215–24.
 39. Wolins NE, Quaynor BK, Skinner JR, et al. S3-12, Adipophilin, and TIP47 package lipid in adipocytes. *J Biol Chem.* 2005;280:19146–55.
 40. Park JK, Coffey NJ, Limoges A, et al. The heterogeneity of lipid metabolism in cancer. *Adv Exp Med Biol.* 2018;1063:33–55.
 41. Nassir F, Wilson B, Han X, et al. CD36 is important for fatty acid and cholesterol uptake by the proximal but not distal intestine. *J Biol Chem.* 2007;282:19493–501.
 42. Son NH, Basu D, Samovski D, et al. Endothelial cell CD36 optimizes tissue fatty acid uptake. *J Clin Investig.* 2018;128:4329–42.
 43. Nath A, Chan C. Genetic alterations in fatty acid transport and metabolism genes are associated with metastatic progression and poor prognosis of human cancers. *Sci Rep.* 2016;6:18669.
 44. Pascual G, Avgustinova A, Mejetta S, et al. Targeting metastasis-initiating cells through the fatty acid receptor CD36. *Nature.* 2017;541:41–45.
 45. Hamid O, Robert C, Daud A, et al. Five-year survival outcomes for patients with advanced melanoma treated with pembrolizumab in KEYNOTE-001. *Ann Oncol.* 2019;30:582–8.
 46. Zecchin KG, Rossato FA, Raposo HF, et al. Inhibition of fatty acid synthase in melanoma cells activates the intrinsic pathway of apoptosis. *Lab Invest.* 2011;91:232–40.
 47. Seguin F, Carvalho MA, Bastos DC, et al. The fatty acid synthase inhibitor orlistat reduces experimental metastases and angiogenesis in B16-F10 melanomas. *Br J Cancer.* 2012;107:977–87.
 48. Dean EJ, Falchook GS, Patel MR, et al. Preliminary activity in the first in human study of the first-in-class fatty acid synthase (FASN) inhibitor, TVB-2640. *J Clin Oncol.* 2016;34:2512–2512. (no. 15_suppl (May 20 2016))
 49. Donizy P, Biecek P, Halon A, et al. Nucleoli cytomorphology in cutaneous melanoma cells—a new prognostic approach to an old concept. *Diagn Pathol.* 2017;12:88.